

Impact of rainfall on *Aedes aegypti* populations

L.D. Valdez^{a,b,c,*}, G.J. Sibona^{a,b}, C.A. Condat^{a,b}

^a Facultad de Matemática, Astronomía, Física y Computación, Universidad Nacional de Córdoba, Ciudad Universitaria, 5000 Córdoba, Argentina

^b Instituto de Física Enrique Gaviola, CONICET, Ciudad Universitaria, 5000 Córdoba, Argentina

^c Center for Polymer Studies, Boston University, Boston, MA 02215, USA

ARTICLE INFO

Keywords:

Aedes
Rainfall
Mosquito abundance
Mathematical modeling
Taiwan

ABSTRACT

Aedes aegypti is the main vector of multiple diseases, such as dengue, Zika, and chikungunya. Due to modifications in weather patterns, its geographical range is continuously evolving. Temperature is a key factor for its expansion into regions with cool winters, but rainfall can also have a strong impact on the colonization of these regions, since larvae emerging after a rainfall are likely to die at temperatures below 10 °C. As climate change is expected to affect rainfall regimes, with a higher frequency of heavy storms and an increase in drought-affected areas, it is important to understand how different rainfall scenarios may shape *Ae. aegypti*'s range. We develop a model for the population dynamics of *Ae. aegypti*, coupled with a rainfall model to study the effect of the temporal distribution of rainfall on mosquito abundance. Using a fracturing process, we then investigate the effect of a higher variability in the daily rainfall. As an example, we show that rainfall distribution is necessary to explain the geographic range of *Ae. aegypti* in Taiwan, an island characterized by rainy winters in the north and dry winters in the south. We also predict that a higher variability in the rainfall time distribution will decrease the maximum abundance of *Ae. aegypti* during the summer. An increase in daily rainfall variability will likewise enhance its extinction probability. Finally, we obtain a nonlinear relationship between dry season duration and extinction probability. These findings can have a significant impact on our ability to predict disease outbreaks.

1. Introduction

The prevalence areas of both emerging and well-established (Hay et al., 2002; Rochlin et al., 2013; Morin and Comrie, 2013; Caminade et al., 2017; Xu et al., 2016) vector-borne diseases are likely to be substantially modified by climate variations. Being *Ae. aegypti* the main vector of several important diseases, its ecology is currently the focus of intense research. Since climate is a key determinant of the mosquito habitat (Hopp and Foley, 2001), climate change is expected to significantly alter its geographic range and put new regions at risk. To predict the future evolution of this range it is necessary to have a clear understanding of how different climatic factors affect *Ae. aegypti*'s thriving and survival. While temperature governs its reproduction, maturation and mortality rates (Bar-Zeev, 1958), rainfalls generate breeding grounds for larvae and pupae (Moore et al., 1978). At variance with other mosquito species, *Ae. aegypti*'s eggs are laid above the water surface and hatch only when the water level rises and wets them. The long survival times of its dry eggs endow *Ae. aegypti* with a competitive advantage over other mosquito species during long periods of drought, but a winter rain may force their hatching and the subsequent larval death. The determination of how climate change may affect the

geographical distribution of this mosquito is thus highly nontrivial. In this paper we address the influence of different rainfall regimes on *Ae. aegypti*.

Aedes aegypti inhabits tropical and subtropical regions worldwide, its geographic range being roughly limited by the 10 °C winter isotherms (Christophers, 1960). The areas close to these isotherms are called “cool margins” (Eisen and Moore, 2013; Eisen et al., 2014). Although the literature describing the reproduction, maturation, and mortality rates, and the dynamics of the mosquito population in warm climates is vast (Tun-Lin et al., 2000; Maciel-De-Freitas et al., 2007; Katyal et al., 1996; Magori et al., 2009), fewer studies have been conducted in the “cool margins”, which often receive cold fronts in winter. Rozeboom (1939) studied the survival of *Ae. aegypti* during the winter in Stillwater, Okla. (USA), where the temperature is often below freezing. This author found that only those *Ae. aegypti* eggs that were protected from rain and snow became vigorous adults. Later on, Tsuda and Takagi (2001) studied the survival of larvae in Nagasaki, Japan, finding that they did not tolerate the low winter temperatures. While Tsuda and Takagi did not perform a direct study with rainfall, they suggested that winter rainfalls could cause mosquito eggs to hatch before spring, and hence the larvae could die due to the low temperatures.

* Corresponding author at: Center for Polymer Studies, Boston University, Boston, MA 02215, USA.

E-mail address: lvaldez@famaf.unc.edu.ar (L.D. Valdez).

Similarly, Chang et al. (2007) found in field studies in Taiwan that larval mortality increases rapidly due to cold fronts. Since rainfall may trigger the hatching process, winter rainfalls could impact negatively on *Ae. aegypti*'s ability to colonize new regions, especially in the “cool margins”. In addition, as climate change is expected not only to increase the temperature but also the frequency of storms and droughts (Easterling et al., 2000), it is important to evaluate how a higher variability in precipitation will affect the dynamics of the mosquito population.

In this work we study the effect of different rainfall regimes on the survival of *Ae. aegypti*, using Taiwan as an example for our description. This island is an excellent case study. Its average summer temperatures are usually above 20 °C and it receives abundant rainfall throughout its territory (Central Weather Bureau, Taiwan, 2017). Taiwan has winter isotherms above 10 °C, although northern temperatures are slightly lower than those in the south. Crucially, the rainfall regime in winter is not spatially homogeneous, due to the presence of the Central Mountain Range (Chen and Chen, 2003). For instance, in January Taipei (located in the north) receives an average rainfall of 83mm, whereas in Kaohsiung (located in the south) the average rainfall is 16mm. On the other hand, despite the small surface of Taiwan, entomological studies indicate that the *Ae. aegypti* population occurs only in the south (Yang et al., 2014; Hwang and Chao, 1991), so we posit that winter rainfall is a determinant for the absence of *Ae. aegypti* in the north of the country.

We calibrate our model of mosquito populations to reproduce the actual geographical distribution of mosquitoes in four representative Taiwanese cities. Our model correctly predicts that *Ae. aegypti* should not be present in Taipei, but thrive in Kaohsiung, but it also predicts that, if we reversed the rainfall data for these two cities we would find that this species would become extinct in Kaohsiung but prosper in Taipei. This result provides a strong validation of our working hypothesis. To find out how different rainfall regimes would impact on the mosquito population dynamics, we present a model to generate synthetic rainfall time series. This model is based on a fracturing method (Finley and Kilkki, 2014), which allows us to modify the temporal distribution of rainfall. Using this rainfall model, we find that the four Taiwanese cities have favorable conditions during the summer for the reproduction of *Ae. aegypti*. In addition, we obtain that, as the variability of rainfall increases, the maximum mosquito abundance M_{max} diminishes. Then, we explore the effect of winter on the survival of *Ae. aegypti*, obtaining that in all cities except Taipei a decrease in rainfall variability reduces the likelihood of mosquito extinction. Additionally, we analyze how mosquitoes would withstand winter in the four cities if the rate of reproduction changed considering the same rainfall regime, and we find that Kaohsiung is still the most favorable city for these mosquitoes. Finally, we study how the duration of the dry period affects mosquito survival, obtaining a nonlinear relationship between these two variables.

2. The model of mosquito abundance

In this section we introduce a climate-driven abundance model of *Ae. aegypti* mosquitoes, using four main compartments: eggs (E_T), larvae (L), pupae (P), and adult mosquitoes (M). In addition, we distinguish between dry (E_D) and wet eggs (E_W). The former are those eggs that have not been in contact with water and therefore cannot hatch, while the latter are those that were in contact with water, which we will assume to come only from rainfall. In our model only wet eggs develop into larvae. In Fig. 1 we show a schematic of the transitions between compartments and in Table 1 we present a summary of the parameters of our model that are related with oviposition and rainfall. In the following, we will explain the dependence of the transition rate coefficients with temperature and rainfall.

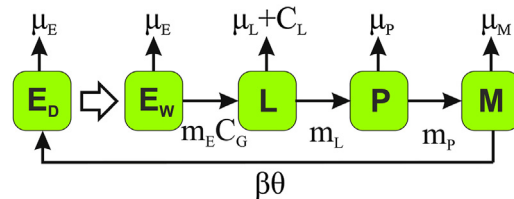


Fig. 1. Schematic representation of the *Ae. aegypti* evolution through different maturation stages. Mosquito compartments are: dry eggs (E_D), wet eggs (E_W), larvae (L), pupae (P), and adult mosquitoes (M). Thin arrows symbolize a waiting time transition which follows an exponential function, whereas the thick arrow represents a delta waiting time distribution from dry eggs to wet eggs (see Section 2.2). The rate β denotes the birth rate of mosquitoes in optimal conditions and $\theta \in [0, 1]$ is a factor that takes into account the effect of temperature on the total birth rate. The rates μ_E , μ_L , μ_P and μ_M represent the mortality rates of the eggs, larvae, pupae and adult mosquitoes, respectively. The rates m_E , m_L and m_p depict the transition between different compartments. The factor C_G represents the “Gillett effect” which delays the hatching process when the larval population increases, and the rate C_L is the larval mortality rate due to overcrowding (see Section 2.3). The dependency of the transition rate from compartment E_D to E_W , and that of the maturation and mortality rates with the temperature and rainfall are described in Sections 2.1–2.4 and in the Appendix.

Table 1

Variables and parameters related with oviposition and rainfall.

Quantity	Definition
β	Birth rate of mosquitoes in optimal conditions (days ⁻¹)
θ	Effect of the temperature on the mosquito birth rate
K_L	Carrying capacity
H_{max}	Maximum daily amount of accumulated rainwater [mm]
H	Accumulated amount of rainwater [mm]
R	Daily rainfall [mm]
$Evap$	Daily evapotranspiration [mm]
k	Constant of the Ivanov model [mm/°C ²] (see Eq. (5))
T	Average daily temperature [°C]
Hum	Daily relative humidity

2.1. Survival of *Ae. aegypti* at low temperatures

Contrary to other *Aedes* species, such as *Ae. albopictus* or *Ae. albifasciatus*, which survive freezing temperatures (Thomas et al., 2012; Krešet al., 2016; Garzón et al., 2013), different studies suggest that *Ae. aegypti* eggs only survive a few hours at low temperatures. For example, Hatchett (1946) found that only 40% of *Ae. aegypti* eggs could hatch after they were immersed in water and exposed to 1°C for 24hs; Chang et al. (2007) found that the larval mortality rate increases rapidly when the minimum temperature is below about 10°C. On the other hand, historical global collections suggest that *Ae. aegypti* is distributed geographically only in areas with winter isotherms above 10°C (Christophers, 1960). Therefore, we will assume in this work that all mosquito compartments that are in contact with water, i.e. wet eggs, larvae, and pupae, lose a 50% of their members at the end of any day that has a minimum temperature below 10°C (see Appendix Section A.4). Above this threshold, the dependence of the mortality rate with the temperature for each compartment is that given by Barmak et al. (2014) (see Appendix Section A.6.3).

2.2. Rainfall and wet eggs

Ae. aegypti lays its eggs on the inner side of containers above the water line (see Ref. (Goddard, 2016)). These eggs are regarded in our model as dry eggs and when they are flooded, for example by rainwater, they usually hatch. Therefore, following the work of Romeo Aznar et al. (2013) and Karl et al. (2014), we propose that, if on day d it rains R millimeters, the fraction of dry eggs that become wet eggs is given by the following Hill function,

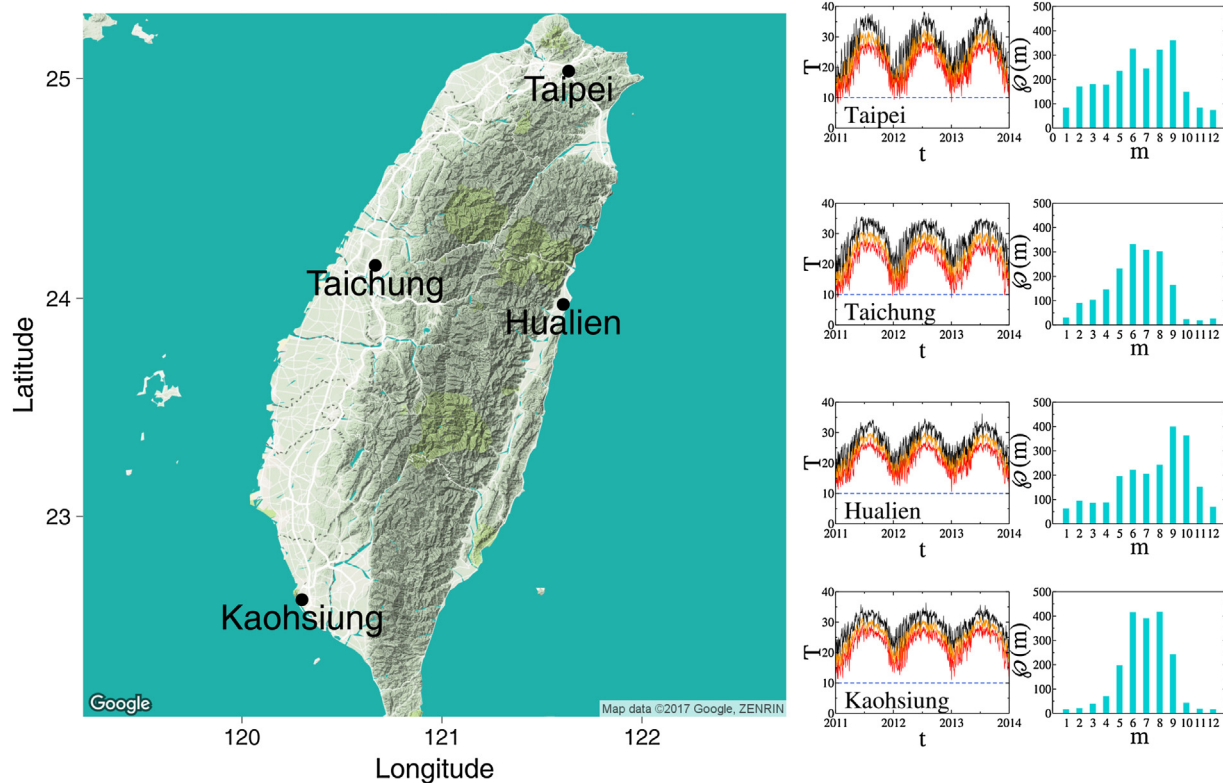


Fig. 2. Left panel: Map showing the four cities of Taiwan for which we apply our mosquito model using a synthetic rainfall time series: Taipei, Taichung, Hualien, and Kaohsiung (Google maps, 2017). Center panels: Maximum (black line), average (orange line) and minimum (red line) temperatures for each city in the period 2011–2013. The horizontal dashed line stands for the 10 °C isotherm. Rightmost panels: Average monthly rainfall $\mathcal{P}(m)$ in the period 1981–2010 (bar plots), with $m = 1$ for January and $m = 12$ for December. (For interpretation of the references to color in this caption, the reader is referred to the web version of this article.)

$$f(R) = 0.8 \frac{(R/R_{\text{thres}})^5}{1 + (R/R_{\text{thres}})^5}. \quad (1)$$

Here, R_{thres} is the rainfall threshold and the prefactor 0.8 stands for the maximum fraction of eggs that may hatch when they are flooded. In this work, we set tentatively $R_{\text{thres}} = 10$ [mm]. No qualitatively significant differences were found when we used $R_{\text{thres}} = 7.5$ [mm] (a figure used by Romeo Aznar et al. (2013)) and $R_{\text{thres}} = 12.5$ [mm] in the computation (results not shown).

This function is applied at the end of day $t = d$ on the dry egg compartment, where t is a continuous variable and d is a non-negative integer (see Appendix Section A.4).

2.3. The Gillett effect and the intraspecific larval competition

Wet eggs hatch at a rate proportional to m_E , which depends only on temperature (see Eq. (A.2)). However, several studies (Gillett, 1955; Gillett et al., 1977) suggested that the hatching process is delayed when the larval population increases, which is called the Gillett effect. In order to introduce this effect in our model, we multiply the rate m_E by

$$C_G = \begin{cases} 1 - \frac{L}{K_L} & \text{if } L < K_L \\ 0 & \text{if } L \geq K_L \end{cases} \quad (2)$$

Therefore, if the number of larvae exceeds the larval capacity K_L then no wet egg can make a transition to the larval compartment. On the other hand, it is known that the larval population growth is restricted by intraspecific competition, which increases the larval death rate. In our model we include this effect by adding to the larval mortality rate c_L the following term (see Ref. (Otero et al., 2006)):

$$c_L = 1.5 \frac{L}{K_L}. \quad (3)$$

2.4. Effect of rainfall on the carrying capacity

The persistence of breeding sites is a key factor for the survival of mosquitoes in the aquatic stage. Rainfall creates breeding sites where larvae develop prior to becoming adult mosquitoes, and evaporation tends to shrink these sites. Therefore, we propose that the carrying capacity depends on the amount of available water $H(t)$, whose variation is defined as follows:

$$H(t+1) = \begin{cases} 0 & \text{if } H(t) + \Delta(t) \leq 0 \\ H_{\max} & \text{if } H(t) + \Delta(t) \geq H_{\max} \\ H(t) + \Delta(t) & \text{otherwise,} \end{cases} \quad (4)$$

where $\Delta(t) = R(t) - Evap(t)$, $R(t)$ is the amount of rain on day t and $Evap(t)$ is the daily evaporation. Note that H can increase only up to a maximum value H_{\max} since we consider that at a higher water level the containers or breeding sites overflow. Besides, following the Ivanov model (Romanenko, 1961; Valipour, 2014), we propose that the evaporation rate $Evap(t)$ is given by the expression,

$$Evap(t) = k(25^{\circ}\text{C} + T(t))^2(100 - Hum(t)). \quad (5)$$

where T is the average temperature and Hum the humidity. Finally, we propose that the carrying capacity is given by:

$$K_L(t) = K_{\max} \frac{H(t)}{H_{\max}} + 1, \quad (6)$$

where K_{\max} is the maximum carrying capacity and the 1 is introduced to avoid divergences when $H(t) \rightarrow 0$ in the Eqs. (2) and (3).

For more details of our model of *Ae. aegypti* mosquitoes see Appendix Section A.6. In the following section we will apply our mosquito model to study the case of Taiwan, using the actual rainfall time series.

Table 2

Estimated values of (β , k , H_{max} , K_{max}) using a Latin hypercube sampling.

Parameter	Values
β [day $^{-1}$]	0.52 [0.25, 1.19]
k [mm/ $^{\circ}$ C 2]	$3.9 \cdot 10^{-5}$ [$3.3 \cdot 10^{-6}$, $6.6 \cdot 10^{-5}$]
H_{max} [mm]	24 [15, 30]
K_{max}	212 [70, 4000]

3. Case study: Taiwan

As mentioned in the Introduction, to study how different rainfall regimes impact on the mosquito population it is informative to analyze the case of Taiwan. More specifically, we will apply our model to study mosquito populations in four cities in Taiwan: Taipei (north), Taichung (west), Hualien (east), and Kaohsiung (south). In Fig. 2 we show their average, minimum, and maximum daily temperatures in the period 2011–2013, and the average monthly precipitation $\mathcal{P}(m)$ in the period 1981–2010. Of these four cities, an established *Ae. aegypti* population has been found only in Kaohsiung. We investigate the reasons why.

In order to model the actual distribution of *Ae. aegypti* in these cities, we calibrate a deterministic version of our model to the time series of adult *Ae. aegypti* abundances per block in Kaohsiung in the period January 2010–December 2012. Namely, we use a Latin hypercube sampling (LHS) method to generate points in a four-dimensional space defined by the vector (β , k , H_{max} , K_{max}). Additionally, since the actual abundance of *Ae. aegypti* populations is negligible or null in Taipei, Taichung, and Hualien, for each point of the LHS method we also compute the mean square distance between the predicted abundance of adult mosquitoes corresponding to each city and a null abundance mosquito series. Finally, we select the point of the LHS that minimizes the sum of the mean square distances for the four cities. See Appendix Section A.3 for more details of the calibration process. In Table 2 we show the estimated values of the parameters¹.

In Fig. 3a we show the actual time series of the abundance of adult mosquitoes (Taiwan CDC, 2017) and the predictions of our model using the parameters obtained with the calibration process and the actual time series of temperature, rainfall, and humidity of Kaohsiung (Central Weather Bureau, Taiwan, 2017). Although our model does not reproduce exactly the heights of the actual mosquito abundance, the positions of the peaks are well correlated with the data. We recall that the Aedes populations in the other cities are extinct.

In order to ascertain if rainfall is indeed responsible for the distribution of *Ae. aegypti* mosquitoes in Taiwan, we computed the dynamics of mosquito abundances in Kaohsiung and Taipei, but *exchanging the actual rainfall time series* between these places. As it can be seen from Fig. 3b, in this hypothetical scenario where Taipei has drier winters, it could maintain a sizable population of mosquitoes through the years. On the other hand, if Kaohsiung had rainy winters, *Ae. aegypti* would become extinct there. These results confirm that our model is effective describing scenarios where rainfall controls the mosquito survival.

In the following sections, we introduce the model to generate synthetic rainfall time series, which will allow us to study how different rain regimes can shape *Ae. aegypti*'s geographic distribution.

4. Synthetic rainfall time series

In order to study the dynamics of mosquito populations for different rainfall regimes, we will use the method to generate synthetic rainfall

time series presented in Ref. (Valdez et al., 2017), which we briefly review next. In this method, we must first specify the total monthly rainfall $\mathcal{P}(m)$ and the monthly number of rainy days $\mathcal{D}(m)$, where m stands for the month. These variables are often used in regression models to predict the number of mosquitoes, as well as to describe the rainfall regime in meteorological forecasting (Norrrant and Douguédroit, 2006; Modarres and da Silva, 2007; Hu et al., 2006; Pascual et al., 2006). The values of $\mathcal{P}(m)$ and $\mathcal{D}(m)$ can either be assigned using the actual averages obtained from meteorological data, or they can be modeled using mathematical functions.

To decide how the monthly rainfall $\mathcal{P}(m)$ for a given month m is distributed on a daily basis, we use a fracturing method which consists in successively decomposing the monthly precipitation $\mathcal{P}(m)$ into the sum of two terms (see Refs. (Finley and Kilkki, 2014; Valdez et al., 2017)), until $\mathcal{P}(m)$ is the sum of $\mathcal{D}(m)$ terms. Namely, this process begins by decomposing $\mathcal{P}(m)$ into two non-negative terms X_1 and X_2 with $\mathcal{P}(m) = X_1 + X_2$, where X_1 is given by

$$X_1 = \mathcal{P}(m) \times \begin{cases} \rho^{\frac{1-\alpha}{\alpha}} & \text{if } 0 \leq \rho < \frac{\alpha}{2} \\ \frac{1}{2} + \left(\rho - \frac{1}{2}\right) \frac{\alpha}{1-\alpha} & \text{if } \frac{\alpha}{2} \leq \rho \leq 1 - \frac{\alpha}{2} \\ 1 - (1-\rho)^{\frac{1-\alpha}{\alpha}} & \text{if } 1 - \frac{\alpha}{2} < \rho \leq 1 \end{cases} \quad (7)$$

where ρ is a uniform random variable and $\alpha \in [0, 1]$ is a parameter that controls the variance of the values of X_1 . In particular, for $\alpha = 0$, $X_1 = X_2 = \mathcal{P}(m)/2$, while for $\alpha = 1$ we obtain $X_1 = 0$ and $X_2 = \mathcal{P}(m)$. Therefore, an increase in the value of α generates a rainfall time series with a higher heterogeneity in the daily amount of precipitation. This step is applied iteratively to each term until the total number of terms is $\mathcal{D}(m)$. Each of these terms corresponds to a total daily rainfall, which is assigned at random to one day of the month.

Although this method allows us to explore different scenarios of rainfall heterogeneity, it is of interest to determine the value of α that best fits an actual rainfall time series, as a reference value for our analysis. To this end, in Appendix Section A.5, we develop a method that computes the value of α that best fits the variance of the daily precipitation for a given period of time (usually, one month).

In Table 3 we show the values of α for a few cities. Notably we obtain that the values are all distributed in a relatively narrow range ([0.32; 0.46]), suggesting that rainfalls are moderately heterogeneous.

4.1. Results with synthetic rainfall time series

In this section we apply the model of synthetic rainfall time series to further analyze the effect of rainfall on the mosquito population in Taiwan. In Fig. 4 we show the maximum peak M_{max} of adult mosquito abundance in the summer of 2011 in Taipei and Kaohsiung; here we use the actual temperature and humidity time series and the synthetic rainfall for various values of α . For simplicity, we use the same value of α for all months. We integrate our mosquito model over a period of one year, setting as initial condition $E_D = E_W = L = P = M = 10$ in May 2011, and we use the average rainfall and the mean number of rainy days per month corresponding to the period 1981–2010 for the synthetic rainfall model. From the figure we observe that the peak of abundance is a decreasing function with the heterogeneity α : since the monthly precipitation is concentrated in fewer days when α increases, the mosquitoes have often a smaller amount of water available to reproduce. Similar plots were obtained for Hualien and Taichung (not shown here).

We also observe that the four cities in Taiwan have favorable conditions for mosquito breeding during the summer. An important question is whether the mosquito population that invades an unoccupied area in spring-summer is able to survive the winter season, at least as dried eggs. To test this, we integrate the mosquito abundance equations over the period May 2011–April 2012 for the four cities and compute

¹ The intervals represent the set of values whose mean square distance error in the calibration process deviate at most by 10% from the optimal mean square distance.

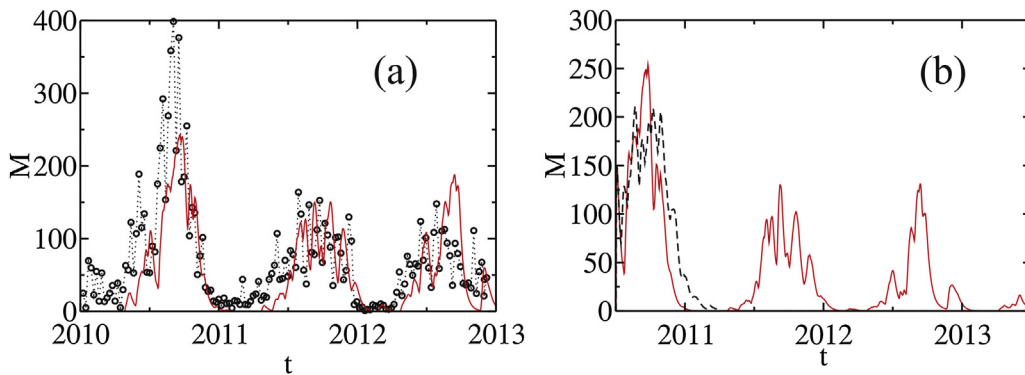


Fig. 3. (a) Time series of the number of adult *Ae. aegypti* mosquitoes obtained from the Kaohsiung data (circles) (Taiwan CDC, 2017) and the prediction of our model (solid line), using the parameters from Table 2 and the actual time series of temperature, rainfall, and humidity for Kaohsiung in the period January 2010–December 2012 (Central Weather Bureau, Taiwan, 2017). For the calibration we have re-scaled the actual time series of adult mosquito abundances, so that this abundance is of 100 mosquitoes in the summer. (b) Evolution of the mosquito abundance

using the calibrated parameters shown in Table 2 and the actual meteorological data of Kaohsiung and Taipei, but where we swapped the rainfall time series of these two cities. The solid red (dashed black) line corresponds to the case of temperature and humidity of Taipei (Kaohsiung) and the rainfall of Kaohsiung (Taipei). (For interpretation of the references to color in this caption, the reader is referred to the web version of this article.)

Table 3

Estimated values of α for several cities. Meteorological data were obtained from Ref. (Hong Kong Observatory, 2017) for the city of Hong Kong, from Ref. (Bureau of Meteorology, Australia, 2017) for the cities in Australia, and from Ref. (The National Oceanic and Atmospheric Administration (NOAA), 2017) for the other cities. In the second column we show the month analyzed, which corresponds to the rainiest month in each city.

Cities (number of years analyzed)	Month analyzed	$\bar{\alpha}$
Sydney, Australia (157 years)	April	0.46
Hong Kong, China (126 years)	June	0.44
Berlin, Germany (134 years)	July	0.39
Atlanta, USA (88 years)	March	0.39
Happy Valley, Australia (46 years)	March	0.38
Los Angeles, USA (91 years)	February	0.38
London, UK (43 years)	October	0.36
Chapingo, Mexico (44 years)	July	0.32

the *Ae. aegypti* extinction probability $Prob(\alpha)$ at the end of April 2012 for different rainfall heterogeneity values α . Note that we consider that a mosquito species is extinct if the number of members in each compartment is null. In Fig. 5a we observe that $Prob(\alpha)$ is an increasing function with α for all the cities, which is consistent with a decreasing of M_{max} with α as it was shown in Fig. 4. Additionally, we plot in Fig. 5b the extinction probability for different values of the oviposition rate β with $\alpha = 0.45$.² In this figure we observe that Kaohsiung is the most favorable city for the establishment of mosquitoes. In turn, we note that the probability $Prob(\beta)$ is vanishingly small for $\beta \gtrsim 0.50 = \beta_c$ in Kaohsiung, which suggests that, in order to model *Ae. aegypti* populations in this city with a synthetic rainfall time series, we should use an oviposition rate β above β_c .

On the other hand, although Taichung is the second city with the driest winter, our model predicts that the second most favorable city for *Ae. aegypti* after Kaohsiung is Hualien, which has slightly warmer winters than Taichung. This suggests that temperature can compensate the negative effect of winter rainfall.

4.2. Why is *Ae. aegypti* not endemic to Hualien?

It is interesting to further discuss the reasons why *Ae. aegypti* is not endemic to Hualien. Having a temperature similar to Kaohsiung and total winter precipitations that are about half those in Taipei (see Fig. 2), Hualien is the second most favorable city for the establishment of *Ae. aegypti*. From Fig. 5 we note that for $0.50 \lesssim \beta \lesssim 0.60$ it would be

² Since we have only 9 years of meteorological data for Kaohsiung, we cannot estimate accurately the value of α for this city, and hence we use $\alpha = 0.45$ as a reference value which is also very close to the one obtained for Hong Kong (see Table 3).

possible to reproduce the real geographic distribution of *Ae. aegypti* in Taiwan. However, if the true value of the oviposition rate β is slightly greater than 0.6, the fact that there are no mosquitoes in Hualien may be due to variables we did not consider in our model, such as competition with other mosquito species (Reiskind and Lounibos, 2009) or local predators. In addition, Han and Chuang (1981) suggested that Hualien presents the highest amount of fungi concentration in the whole country, due to Asian dust storms. For instance, fungal traps in this city revealed the presence of *Periconia* and *Torula* (see Ref. (Ho et al., 2005)). Notably, a recent study found that similar fungi were the cause of mortality of *Ae. aegypti* eggs in Chaco, Argentina (see Ref. (Giménez et al., 2015)).

4.3. Extinctions and dry season length

Another relevant aspect of a particular rainfall regime is how the duration of the dry season affects the establishment and survival of *Ae. aegypti* in a city. To study this effect, we will use a model of synthetic rainfall time series in which the amount of monthly rainfall $\mathcal{P}(m)$ and the number of rainy days $\mathcal{D}(m)$ are given by the following functions,

$$\mathcal{P}(m) = (P_{\max} - P_{\min}) \left(\frac{1}{2} + \frac{1}{2} \cos \left(\frac{2\pi}{12} (m - m_0) \right) \right)^{\gamma} + P_{\min}, \quad (8)$$

$$\mathcal{D}(m) = (D_{\max} - D_{\min}) \left(\frac{1}{2} + \frac{1}{2} \cos \left(\frac{2\pi}{12} (m - m_0) \right) \right)^{\gamma} + D_{\min}, \quad (9)$$

where $\gamma \in [0, \infty)$ controls the duration of the dry season (the higher the γ , the longer the duration of the dry season); m_0 is the rainiest month of the year, P_{\max} is the total precipitation in the rainiest month (in millimeters), and P_{\min} that in the driest month. The variables D_{\max} and D_{\min} have similar interpretations for the number of rainy days. Note that $\mathcal{P}(m_0) = P_{\max}$ and $\mathcal{D}(m_0) = D_{\max}$ for all values of γ . Analogously, $\mathcal{P}(m_0 - 6) = P_{\min}$ and $\mathcal{D}(m_0 - 6) = D_{\min}$ for all values of γ . Here, we set $m_0 = 7$ (July). Since the number of rainy days is an integer number but in Eq. (9) $\mathcal{D}(m)$ is a real number, for each rainfall time series realization we choose the number of rainy days to be $[\mathcal{D}(m)]$ and $[\mathcal{D}(m)] + 1$ with probabilities $\mathcal{D}(m) - [\mathcal{D}(m)]$ and $1 - (\mathcal{D}(m) - [\mathcal{D}(m)])$, respectively (here $[\dots]$ stands for the integer part).

In Fig. 6a we show the probability of extinction of *Ae. aegypti* for each month as a function of γ , for $\alpha = 0.45$. In Appendix Section A.2 we show the same plot for $\alpha = 0.10$ and 0.80 ; in all cases we use the actual temperature and humidity time series of Taipei. We observe that for low values of γ , that is to say, when the amount of precipitation is high in almost every month, the extinction occurs in winter. This is consistent with the Tsuda and Takagi's hypothesis, which states that winter rainfall could cause eggs to hatch in a period with low temperatures (see the Introduction). As γ increases, the maximum probability of

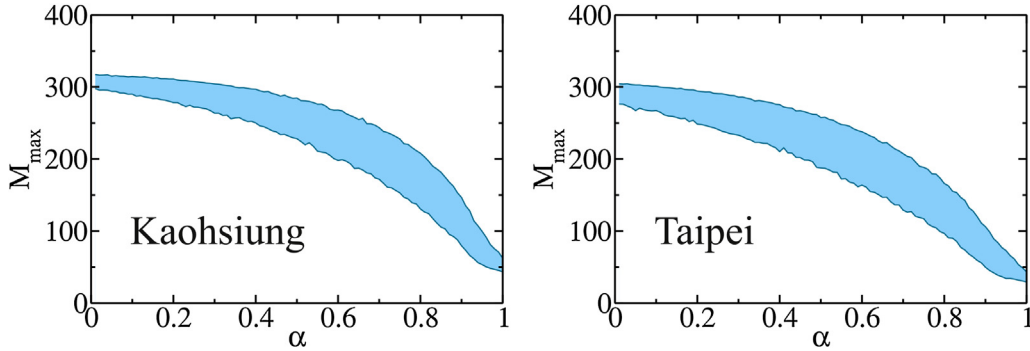


Fig. 4. M_{max} as a function of α using the actual temperature and humidity data for the period May 2011–April 2012. Light blue region: 90% of the 1000 realizations for the synthetic rainfall using the average rainfall and the mean number of rainy days per month corresponding to the period 1981–2010 (see Fig. 2). (For interpretation of the references to color in this caption, the reader is referred to the web version of this article.)

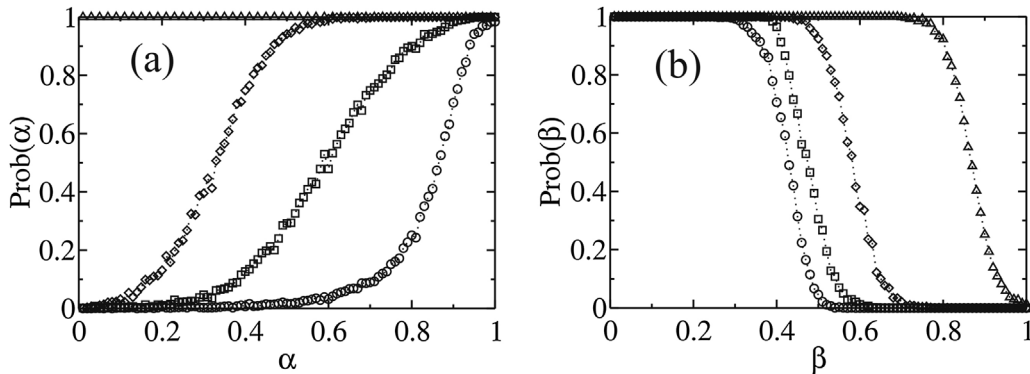


Fig. 5. *Aedes aegypti* extinction probabilities in Kaohsiung (circles), Hualien (squares), Taichung (diamonds), and Taipei (triangles) as (a) functions of α using the calibrated values of Table 2; and (b) as functions of β with $\alpha = 0.45$. Dotted lines serve as a guide to the eye. The results are averaged over 1000 realizations of the synthetic rainfall model.

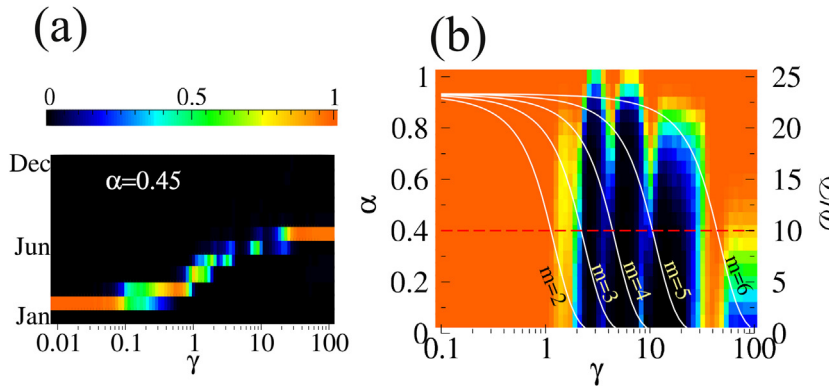


Fig. 6. Effect of the dry period on the extinction probability. Using the model of synthetic rainfall time series, we compute (a) the probability of extinction of mosquitoes for each month in Taipei as a function of γ for $\alpha = 0.45$, and (b) the cumulative probability of extinction of *Ae. aegypti* in Taipei for different values of α and γ . We compute the cumulative probability of extinction after the second year from the date of the initial condition. Panel (b) also shows the average amount of precipitation in a rainy day $\mathcal{P}(m)/\mathcal{D}(m)$ (solid white lines) for $m = 2, 3, 4, 5, 6$ and the rainfall threshold $R_{thres} = 10 (see Eq. (1) and dashed red line). The monthly rainfall distribution and the number of rainy days follow Eqs. (8) and (9). We set: $P_{max} = 350$, $P_{min} = 0$, $D_{max} = 15$, $D_{min} = 1$, and $m_0 = 7$. The initial condition is $E_D = E_W = L = P = M = 10$ on May 1, 2011 and we model the dynamics of mosquito abundance for four years. Cold colors represent a low probability of extinction (black corresponds to a null probability) and warm colors a probability close to 1. The results are averages obtained over 1000 realizations of rainfall time series. (For interpretation of the references to color in this caption, the reader is referred to the web version of this article.)$

extinction moves forward in time: dry periods are longer and more intense. Finally, for the highest values of γ , the extinction occurs in summer: since the (extremely) dry season lasts almost 11 months, very few viable eggs survive until the (short) wet season; these cannot sustain a mosquito population after a rainfall event. Note that extinctions never occur in the fall.

In Fig. 6b we show the effect of the daily rainfall heterogeneity (α) and the duration of the dry season (γ) on the cumulative probability of extinction of *Ae. aegypti* in the city of Taipei. Again, we use the actual temperature and humidity time series of Taipei. We obtain, as expected, that for very low values of γ mosquitoes become rapidly extinct since rainfalls are abundant throughout the year. It should be noted that the probability of extinction does not depend on the daily rainfall variability (α). Therefore, when there is no dry season, the amount of monthly rainfall (in millimeters) is a sufficient predictor for determining

the absence of mosquitoes. However, as γ increases, we observe that the probability of extinction drops, and hence in this parameter domain we can consider that Taipei resembles Kaohsiung. The dry winter allows a bigger egg population to survive; when they hatch in the rainy season the temperature is already high enough to allow these eggs to prosper. Additionally, in this case the probability of extinction also depends on α . This suggests that in areas with dry winter months but without a permanent *Ae. aegypti* population, the role of the variability in the daily precipitation as an explanatory variable for these extinction cases should be further explored.

On the other hand, note that as γ grows for a fixed value of α , the extinction probability increases and decreases several times. In Fig. 6b we show that local transitions from high to low extinction probabilities take place when the average amount of precipitation in a rainy day on month m , i.e. $\mathcal{P}(m)/\mathcal{D}(m)$ is approximately equal to the rainfall

threshold (see Eq. (1)). An extinction may occur, for instance, in a month when rainfalls can flood a certain quantity of eggs but the amount of available water is not enough to sustain a larval population; as γ increases this month will become a “dry” month, so the probability of extinction diminishes because fewer eggs hatch under detrimental conditions. Finally, for very high values of γ , the extinction probability again increases, which is consistent with the results shown in Fig. 6a for a very dry region.

5. Summary

Since *Ae. aegypti* is expanding its territory, potentially contributing to the spread of diseases such as dengue, yellow fever, chikungunya and Zika (Gubler, 2004; Pialoux et al., 2007; Zhang et al., 2017) to new areas, it is important to assess how different climatic variables can shape the present and future geographic ranges of this mosquito. We have developed a model for the *Ae. aegypti* population that takes into account the susceptibility of its immature stages to winter rains. We hypothesize that locations with cool, rainy winters are inimical to this species and test the model by applying it to four cities in Taiwan, reproducing the observed presence (or absence) of *Ae. aegypti*. In particular, we find that the reason *Ae. aegypti* is endemic to Kaohsiung is that it is the city with the lowest precipitation in winter. We also introduce a procedure to generate rainfall time series to explore the effect of

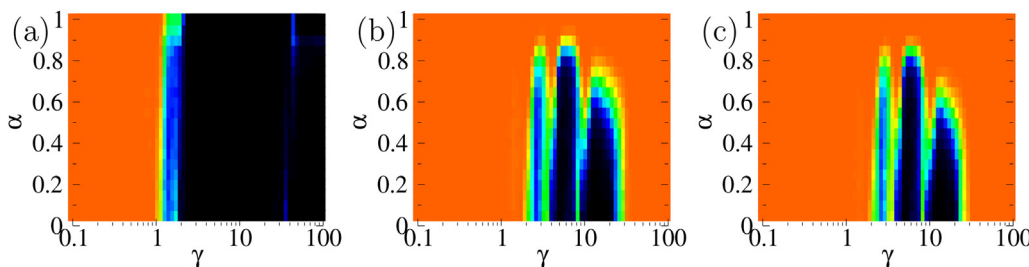
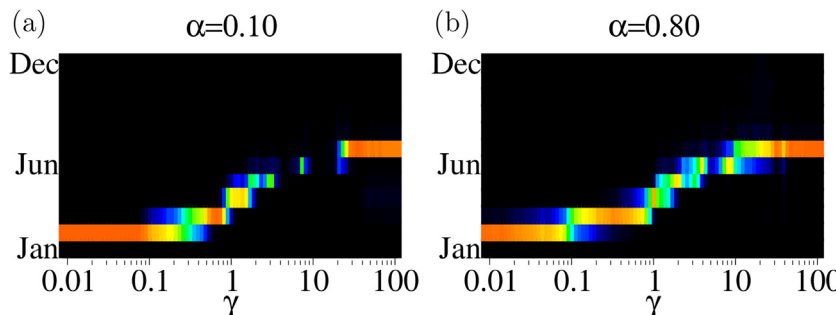
Appendix A

A.1 Research data and code

The source code of our model is available at <https://github.com/LDVal/ImpactOfRainfallOnAedesPopulations>.

A.2 Effect of the dry season on *Ae. aegypti*

Figs. A1 and A2



probability of extinction after one (a), three (b) and four (c) years. The colors have the same meaning as in Fig. 6. (For interpretation of the references to color in this caption, the reader is referred to the web version of this article.)

different rainfall regimes.

Applying our rainfall model to Taiwan, we find that as the precipitation heterogeneity (α) increases, the peak of mosquito abundance during the summer decreases. On the other hand, a reduction in the heterogeneity of daily rainfall decreases the probability of extinction in all the cities, except Taipei. We also obtain that the presence or absence of *Ae. aegypti* depends on a delicate balance between different climatic variables in the regions near the 10 °C winter isotherms.

Finally, we studied the effect of dry season duration on mosquito survival and found that, as it increases, the survival probability also increases. However, because eggs become gradually nonviable, for very long droughts, the likelihood of extinction rises again.

Given that climate change is likely to make the world wetter, predicting the evolution of the geographical habitat of *Ae. aegypti* is not easy: while an increase in the temperature should shift its boundaries towards higher latitudes, an increase in the winter rainfall would be detrimental to its enlargement. The model presented here can be useful to address this challenge.

Acknowledgements

This work was supported by SECyT-UNC (projects 103/15 and 313/16) and CONICET (PIP 11220150100644). We also thank Mgter. Laura López for useful discussions.

Fig. A1. Probability of extinction of mosquitoes for each month in Taipei as a function of γ , using the model of synthetic rainfall time series for two α values: 0.10 and 0.80. The monthly rainfall distribution and the number of rainy days follow Eqs. (8) and (9). We chose: $P_{max} = 350$, $P_{min} = 0$, $D_{max} = 15$, $D_{min} = 1$, and $m_0 = 7$. The initial condition is $E_D = E_W = L = P = M = 10$ on May 1, 2011. We model the dynamics of mosquito abundance for four years. Cold colors represent a low probability of extinction (black corresponds to a null probability) and warm colors a probability close to 1. The results were averaged over 1000 realizations of rainfall time series. (For interpretation of the references to color in this caption, the reader is referred to the web version of this article.)

Fig. A2. Cumulative probability of extinction of *Ae. aegypti* in Taipei for different values of α and γ , using the model of synthetic rainfall time series. The monthly rainfall distribution and the number of rainy days follow Eqs. (8) and (9). We chose: $P_{max} = 350$, $P_{min} = 0$, $D_{max} = 15$, $D_{min} = 1$, and $m_0 = 7$. The initial condition is $E_D = E_W = L = P = M = 10$ on May 1, 2011. We compute the cumulative

A.3 Model calibration

For the calibration of our mosquito population model, we use a Latin hypercube sampling method for the parameters β , k , H_{max} , and K_{max} , and compute the mean square distance between the predicted abundance of mosquitoes and the actual weekly adult mosquito abundance data of Kaohsiung in the period January 2010 – December 2012 (obtained from Ref. (Taiwan CDC, 2017)). Since in Refs. (Romeo Aznar et al. (2013)) and (Karl et al. (2014)) the maximum number of mosquitoes is of the order of 100 per block, we re-scaled the actual abundance data, so it is about 100 mosquitoes per block in the summer. We set as initial conditions, $E_D = E_W = L = P = M = 100$. For the same set of points, we repeat the process for Taipei, Taichung, and Hualien.³ In all the cases, we start the integration six months before the time from which we compute the mean square distance, in order to minimize the effect of the initial conditions. Note that we use the actual values of temperature, humidity, and rainfall for the calibration process. Finally, we choose the point $(\beta, k, H_{max}, K_{max})$ that minimizes the sum of the square distances corresponding to all the cities.

A.4 Integration of the equations of our model

We model a system of compartmental difference-differential equations which we integrate numerically using the Euler method with $\Delta t = 0.01$, where t is given in days. If for any time step the population of a compartment is negative, then we change its value to 0. Since the time series of temperature, humidity and rainfall are on a daily time scale, all the parameters that depend on these variables are considered constant between days d and $d + 1$, i.e. for $t \in [d, d + 1]$, where d is a non-negative integer number. These parameters are calculated using the values of temperature, humidity, and rainfall for that day. In turn, if it rains on day d , then at the end of each rainy day, i.e. when $t = d + 1 - \Delta t$, a fraction of dry eggs go wet as it is explained in Section 2.2. Similarly, if on day d the minimum temperature is below 10 °C, then at time $t = d + 1 - \Delta t$ we apply the rules explained in Section 2.1. Finally, to incorporate the fact that we model discrete populations and to be able to explore extinction processes, we will impose that if the population of a compartment is less than 1 at the end of the integration step $t = d - \Delta t$, then we change its value to 0.

A.5 Calibration of α

In order to compute the value of α that best fits the actual rainfall time series, we propose a procedure based on the distance minimization between the variance of the actual rainfall time series and that of the synthetic one. Namely, we propose the following steps:

1. We calculate the total precipitation \mathcal{P} (in millimeters) and the number of rainy days \mathcal{D} in a period of time (for instance, 30 days) and the variance of the actual daily rainfall. We exclude non-rainy days from the computation of this variance.
2. We use the fracturing process for different values of $\alpha \in [0, 1]$ using the actual values of the total rainfall and the number of rainy days computed in the previous step. Then we measure the variance of the synthetic rainfall series. This step is repeated 10^5 times for each value of α .
3. We choose the value of α that minimizes the distance between the average variance of the synthetic rainfall and the variance of the actual rainfall time series.

To ascertain if this procedure allows us to re-obtain a preset value of α for a synthetic rainfall time series, we generate these series for different values of α and then we apply the method described above. In Table A1 we show that, although our method slightly underestimates the values of α , the new values are close enough to the preset ones to confirm the consistency of the procedure.

Table A1
Estimated values of α for various synthetic rainfall time series.
We constructed 100 of these series for each preset value of α using a total precipitation of $\mathcal{P} = 200$ and $\mathcal{D} = 10$ rainy days in a period of 30 days.

α (preset value)	$\bar{\alpha}$ (estimated value)
0.2	0.16
0.3	0.27
0.4	0.35
0.45	0.42
0.5	0.45
0.6	0.58

A.6 Transition rates

A.6.1 The impact of mean daily temperature on oviposition

We propose that the number of dry eggs laid per unit time is proportional to: (1) the number of adult mosquitoes, (2) the oviposition rate β in optimal conditions of temperature, and (3) a factor $\theta \in [0, 1]$, which stands for the effect of temperature on oviposition. In this work, θ is given by

$$\theta(t) = \begin{cases} 0.1137(-5.4 + 1.8T - 0.2124T^2 + 0.01015T^3 - 0.0001515T^4) & \text{if } 11.7 < T(t) < 37.2 \\ 0 & \text{otherwise,} \end{cases} \quad (\text{A.1})$$

Here the relation between θ and the mean daily temperature T was obtained by Yang et al. on the basis of temperature laboratory experiments (see Refs. (Yang et al., 2009; Lourenço and Recker, 2014)), and the prefactor 0.1137 normalizes θ .

³ For the calibration in Taipei and Kaohsiung, we integrate our equations over the period January 2010–December 2012. For Hualien and Taichung we adjust our model in the period January 2011–December 2012, since the data of temperature and humidity in 2009 are not available.

A.6.2 Maturation rates

In Table A2 we define the maturation rates m_X (where $X = E, L$, and P stand for eggs, larvae, and pupae, respectively). Equation (A.2) defines their relation with the mean daily temperature.

$$m_X = R_X \frac{T + T_0}{298} \frac{\exp\left[\frac{\Delta H_A}{R_0}\left(\frac{1}{298} - \frac{1}{T + T_0}\right)\right]}{1 + \exp\left[\frac{\Delta H_H}{R_0}\left(\frac{1}{T_{1/2}} - \frac{1}{T + T_0}\right)\right]} \quad (\text{A.2})$$

Table A2

Notation and definitions of the maturation rate coefficients.

Quantity	Definition	Value
m_E	rate at which eggs develop into larvae (days ⁻¹)	Eq. (A.2)
m_L	rate at which larvae develop into pupae (days ⁻¹)	Eq. (A.2)
m_P	rate at which pupae develop into mosquitoes (days ⁻¹)	Eq. (A.2)

(see Ref. (Barmak et al., 2014) and references therein), where T is the mean temperature (in Celsius), $T_0 = 273.15$ °C, and R_0 is the universal gas constant. The other parameters (R_X , ΔH_A , ΔH_H , $T_{1/2}$) are shown in Table A3 for $X = E, L$, and P .

Table A3

Values of R_X , ΔH_A , ΔH_H , and $T_{1/2}$ for eggs, larvae and pupae.

X	R_X	ΔH_A	ΔH_H	$T_{1/2}$
E	0.24	10,798	100,000	14,184
L	0.2088	26,018	55,990	304.6
P	0.384	14,931	-472,379	148

In addition, we set the maturation rate coefficient for *Ae. aegypti* larvae to be equal to zero for $T < 13.4$ °C (see Refs. (Chen and Huang, 1988; Chang et al., 2007)).

A.6.3 Mortality rates

In Table A4 we define the mortality rates and their relation with temperature (see Ref. (Barmak et al., 2014) and references therein).

Table A4

Mortality rate coefficients.

Quantity	Definition	Value
μ_E	egg mortality rate (days ⁻¹)	0.011
μ_L	larva mortality rate (days ⁻¹)	0.01 + 0.9725 exp(-(T - 4.85)/2.7035)
μ_P	pupa mortality rate (days ⁻¹)	0.01 + 0.9725 exp(-(T - 4.85)/2.7035)
μ_M	mosquito mortality rate (days ⁻¹)	0.091

References

- Bar-Zeev, M., 1958. The effect of temperature on the growth rate and survival of the immature stages of *Aedes aegypti* (L.). Bull. Entomol. Res. 49 (1), 157–163. <https://doi.org/10.1017/S0007485300053499>.
- Barmak, D.H., Dorso, C.O., Otero, M., Solari, H.G., 2014. Modelling interventions during a dengue outbreak. Epidemiol. Infect. 142 (03), 545–561. <https://doi.org/10.1017/S0950268813001301>.
- Bureau of Meteorology, Australia, 2017. <http://www.bom.gov.au> (accessed 12.04.17).
- Caminade, C., Turner, J., Metelmann, S., Hesson, J.C., Blagrove, M.S., Solomon, T., Morse, A.P., Baylis, M., 2017. Global risk model for vector-borne transmission of Zika virus reveals the role of El Niño 2015. Proc. Natl. Acad. Sci. U. S. A. 114 (1), 119–124. <https://doi.org/10.1073/pnas.1614303114>.
- Central Weather Bureau, Taiwan, 2017. Retrieved from <http://www.cwb.gov.tw/> (accessed 17.05.17).
- Chang, L.-H., Hsu, E.-L., Teng, H.-J., Ho, C.-M., 2007. Differential survival of *Aedes aegypti* and *Aedes albopictus* (Diptera: Culicidae) larvae exposed to low temperatures in Taiwan. J. Med. Entomol. 44 (2), 205–210. [https://doi.org/10.1603/0022-2585\(2007\)44\[205:DSOAAA\]2.0.CO;2](https://doi.org/10.1603/0022-2585(2007)44[205:DSOAAA]2.0.CO;2).
- Chen, C., Huang, C., 1988. Ecological studies on *Aedes aegypti* and *Ae. albopictus* I. Comparison of development threshold and life tables. Yushania 5, 1–15.
- Chen, C.-S., Chen, Y.-L., 2003. The rainfall characteristics of Taiwan. Mon. Weather Rev. 131 (7), 1323–1341. [https://doi.org/10.1175/1520-0493\(2003\)131<1323:TRCOT>2.0.CO;2](https://doi.org/10.1175/1520-0493(2003)131<1323:TRCOT>2.0.CO;2).
- Christophers, S., 1960. *Aedes aegypti* (L.) the Yellow Fever Mosquito: Its Life History, Bionomics and Structure. Cambridge University Press.
- Easterling, D.R., Meehl, G.A., Parmesan, C., Changnon, S.A., Karl, T.R., Mearns, L.O., 2000. Climate extremes: observations, modeling, and impacts. Science 289 (5487), 2068–2074. <https://doi.org/10.1126/science.289.5487.2068>.
- Eisen, L., Monaghan, A.J., Lozano-Fuentes, S., Steinhoff, D.F., Hayden, M.H., Bieringer, P.E., 2014. The impact of temperature on the bionomics of *Aedes (Stegomyia) aegypti*, with special reference to the cool geographic range margins. J. Med. Entomol. 51 (3), 496–516. <https://doi.org/10.1603/ME13214>.
- Eisen, L., Moore, C.G., 2013. *Aedes (Stegomyia) aegypti* in the continental United States: a vector at the cool margin of its geographic range. J. Med. Entomol. 50 (3), 467–478.

- [https://doi.org/10.1603/ME12245.](https://doi.org/10.1603/ME12245)
- Finley, B.J., Kilkki, K., 2014. Exploring empirical rank-frequency distributions longitudinally through a simple stochastic process. PLOS ONE 9 (4), e94920. <https://doi.org/10.1371/journal.pone.0094920>.
- Garzón, M., Jensen, O., Schweigmann, N., 2013. Resistance to freezing temperatures in *Aedes (Ochlerotatus) albifasciatus* (Macquart) eggs (Diptera: Culicidae) from two different climatic regions of Argentina. J. Vector Ecol. 38 (2), 339–344. <https://doi.org/10.1111/j.1948-7134.2013.12049.x>.
- Gillett, J.D., 1955. Variation in the hatching-response of *Aedes* eggs (Diptera: Culicidae). Bull. Entomol. Res. 46 (2), 241–254. <https://doi.org/10.1017/S0007485300030881>.
- Gillett, J.D., Roman, E.A., Phillips, V., 1977. Erratic hatching in *Aedes* eggs: a new interpretation. Proc. R. Soc. Lond. B: Biol. Sci. 196 (1123), 223–232. <https://doi.org/10.1098/rspb.1977.0038>.
- Giménez, J.O., Fischer, S., Zalazar, L., Stein, M., 2015. Cold season mortality under natural conditions and subsequent hatching response of *Aedes (Stegomyia) aegypti* (Diptera: Culicidae) eggs in a subtropical city of Argentina. J. Med. Entomol. 52 (5), 879–885. <https://doi.org/10.1093/jme/tjv107>.
- Goddard, J., 2016. Physician's Guide to Arthropods of Medical Importance. CRC Press/Taylor & Francis Group.
- Google maps, 2017. Retrieved from <http://maps.google.com> (accessed 10.08.17).
- Gubler, D.J., 2004. The changing epidemiology of yellow fever and dengue, 1900 to 2003: full circle? Comp. Immunol. Microbiol. Infect. Dis. 27 (5), 319–330. <https://doi.org/10.1016/j.cimid.2004.03.013>.
- Han, S.H., Chuang, Y.C., 1981. Air-borne fungal spore counts in Taiwan. Chin. Med. J. 28, 193–196.
- Hatchett, S.P., 1946. Winter survival of *Aedes aegypti* (L.) in Houston. Tex. Public Health Rep. (1896–1970) 61, 1234–1244. <https://doi.org/10.2307/4585803>.
- Hay, S.I., Cox, J., Rogers, D.J., Randolph, S.E., Stern, D.I., Shanks, G.D., Myers, M.F., Snow, R.W., 2002. Climate change and the resurgence of malaria in the East African highlands. Nature 415 (6874), 905–909. <https://doi.org/10.1038/415905a>.
- Ho, H.-M., Rao, C.Y., Hsu, H.-H., Chiu, Y.-H., Liu, C.-M., Chao, H.J., 2005. Characteristics and determinants of ambient fungal spores in Huilien, Taiwan. Atmos. Environ. 39 (32), 5839–5850. <https://doi.org/10.1016/j.atmosenv.2005.06.034>.
- Hong Kong Observatory, 2017. <http://www.weather.gov.hk> (accessed 30.05.17).
- Hopp, M.J., Foley, J.A., 2001. Global-scale relationships between climate and the dengue fever vector, *Aedes aegypti*. Clim. Change 48 (2), 441–463. <https://doi.org/10.1023/A:1010717502442>.
- Hu, W., Tong, S., Mengersen, K., Oldenburg, B., 2006. Rainfall, mosquito density and the transmission of Ross River virus: a time-series forecasting model. Ecol. Model. 196 (3), 505–514. <https://doi.org/10.1016/j.ecolmodel.2006.02.028>.
- Hwang, J., Chao, J., 1991. Ecology of *Aedes* mosquitoes and their relationships with dengue epidemics in Taiwan. Chin. J. Entomol. 6, 105–127.
- Karl, S., Halder, N., Kelso, J.K., Ritchie, S.A., Milne, G.J., 2014. A spatial simulation model for dengue virus infection in urban areas. BMC Infect. Dis. 14 (1), 447. <https://doi.org/10.1186/1471-2334-14-447>.
- Katyai, R., Gill, K.S., Kumar, K., 1996. Seasonal variations in *Aedes aegypti* population in Delhi, India. Dengue Bull. 20, 78.
- Kreß, A., Kuch, U., Oehlmann, J., Müller, R., 2016. Effects of diapause and cold acclimation on egg ultrastructure: new insights into the cold hardiness mechanisms of the Asian tiger mosquito *Aedes (Stegomyia) albopictus*. J. Vector Ecol. 41 (1), 142–150. <https://doi.org/10.1111/jvec.12206>.
- Lourenço, J., Recker, M., 2014. The 2012 Madeira dengue outbreak: epidemiological determinants and future epidemic potential. PLoS Negl. Trop. Dis. 8 (8), e3083. <https://doi.org/10.1371/journal.pntd.0003083>.
- Maciel-De-Freitas, R., Torres Codeco, C., Lourenco-De-Oliveira, R., 2007. Daily survival rates and dispersal of *Aedes aegypti* females in Rio de Janeiro, Brazil. Am. J. Trop. Med. Hyg. 76 (4), 659–665. <https://doi.org/10.4269/ajtmh.2007.76.659>.
- Magori, K., Legros, M., Puente, M.E., Focks, D.A., Scott, T.W., Lloyd, A.L., Gould, F., 2009. Skeeter Buster: a stochastic, spatially explicit modeling tool for studying *Aedes aegypti* population replacement and population suppression strategies. PLoS Negl. Trop. Dis. 3 (9), e508. <https://doi.org/10.1371/journal.pntd.0000508>.
- Modarres, R., da Silva, V.d.P.R., 2007. Rainfall trends in arid and semi-arid regions of Iran. J. Arid Environ. 70 (2), 344–355. <https://doi.org/10.1016/j.jaridenv.2006.12.024>.
- Moore, C.G., Cline, B.L., Ruiz-Tibén, E., Lee, D., Romney-Joseph, H., Rivera-Correa, E., 1978. *Aedes aegypti* in Puerto Rico: environmental determinants of larval abundance and relation to dengue virus transmission. Am. J. Trop. Med. Hyg. 27 (6), 1225–1231.
- <https://doi.org/10.4269/ajtmh.1978.27.1225>.
- Morin, C.W., Comrie, A.C., 2013. Regional and seasonal response of a West Nile virus vector to climate change. Proc. Natl. Acad. Sci. U. S. A. 110 (39), 15620–15625. <https://doi.org/10.1073/pnas.1307135110>.
- Norrant, C., Douguédroit, A., 2006. Monthly and daily precipitation trends in the Mediterranean (1950–2000). Theor. Appl. Climatol. 83 (1), 89–106. <https://doi.org/10.1007/s00704-005-0163-y>.
- Otero, M., Solari, H.G., Schweigmann, N., 2006. A stochastic population dynamics model for *Aedes aegypti*: formulation and application to a city with temperate climate. Bull. Math. Biol. 68 (8), 1945–1974. <https://doi.org/10.1007/s11538-006-9067-y>.
- Pascual, M., Ahumada, J.A., Chaves, L.F., Rodo, X., Bouma, M., 2006. Malaria resurgence in the East African highlands: temperature trends revisited. Proc. Natl. Acad. Sci. U. S. A. 103 (15), 5829–5834. <https://doi.org/10.1073/pnas.0508929103>.
- Pialoux, G., Gaizière, B.-A., Jaureguiberry, S., Strobel, M., 2007. Chikungunya, an epidemic arbovirosis. Lancet Infect. Dis. 7 (5), 319–327. [https://doi.org/10.1016/S1473-3099\(07\)70107-X](https://doi.org/10.1016/S1473-3099(07)70107-X).
- Reiskind, M., Lounibos, L., 2009. Effects of intraspecific larval competition on adult longevity in the mosquitoes *Aedes aegypti* and *Aedes albopictus*. Med. Vet. Entomol. 23 (1), 62–68. <https://doi.org/10.1111/j.1365-2915.2008.00782.x>.
- Rochlin, I., Ninivaggi, D.V., Hutchinson, M.L., Farajollahi, A., 2013. Climate change and range expansion of the Asian tiger mosquito (*Aedes albopictus*) in Northeastern USA: implications for public health practitioners. PLOS ONE 8 (4), e60874. <https://doi.org/10.1371/journal.pone.0060874>.
- Romanenko, V., 1961. Computation of the autumn soil moisture using a universal relationship for a large area. Proceedings Ukrainian Hydrometeorological Research Institute (Kiev) 3 12–25.
- Romeo Aznar, V., Otero, M., De Mayo, M.S., Fischer, S., Solari, H.G., 2013. Modeling the complex hatching and development of *Aedes aegypti* in temperate climates. Ecol. Model. 253, 44–55. <https://doi.org/10.1016/j.ecolmodel.2012.12.004>.
- Rozeeboom, L.E., 1939. The overwintering of *Aedes aegypti* L. in Stillwater, Oklahoma. In: Proc. Okla. Acad. Sci., Vol. 19. Norman, Okla. pp. 81.
- Taiwan CDC, 2017. <https://data.cdc.gov.tw/en/> (accessed 31.05.17).
- The National Oceanic and Atmospheric Administration (NOAA), 2017. Retrieved from <http://www.noaa.gov/> (accessed 12.09.17).
- Thomas, S.M., Obermayr, U., Fischer, D., Kreyling, J., Beierkuhnlein, C., 2012. Low-temperature threshold for egg survival of a post-diapause and non-diapause European aedine strain, *Aedes albopictus* (Diptera: Culicidae). Parasites Vectors 5 (1), 100. <https://doi.org/10.1186/1756-3305-5-100>.
- Tsuda, Y., Takagi, M., 2001. Survival and development of *Aedes aegypti* and *Aedes albopictus* (Diptera: Culicidae) larvae under a seasonally changing environment in Nagasaki, Japan. Environ. Entomol. 30 (5), 855–860. <https://doi.org/10.1603/0046-225X-30.5.855>.
- Tun-Lin, W., Burkot, T.R., Kay, B.H., 2000. Effects of temperature and larval diet on development rates and survival of the dengue vector *Aedes aegypti* in north Queensland, Australia. Med. Vet. Entomol. 14 (1), 31–37. <https://doi.org/10.1046/j.1365-2915.2000.00207.x>.
- Valdez, L.D., Sibona, G.J., Diaz, L.A., Contigiani, M.S., Condat, C.A., 2017. Effects of rainfall on Culex mosquito population dynamics. J. Theor. Biol. 421, 28–38. <https://doi.org/10.1016/j.jtbi.2017.03.024>.
- Valipour, M., 2014. Application of new mass transfer formulae for computation of evapotranspiration. J. Appl. Water Eng. Res. 2, 33–46. <https://doi.org/10.1080/23249676.2014.923790>.
- Xu, L., Stige, L.C., Chan, K.-S., Zhou, J., Yang, J., Sang, S., Wang, M., Yang, Z., Yan, Z., Jiang, T., et al., 2016. Climate variation drives dengue dynamics. Proc. Natl. Acad. Sci. U. S. A. 114, 113–118. <https://doi.org/10.1073/pnas.1618558114>.
- Yang, C.-F., Hou, J.-N., Chen, T.-H., Chen, W.-J., 2014. Discriminable roles of *Aedes aegypti* and *Aedes albopictus* in establishment of dengue outbreaks in Taiwan. Acta Trop. 130, 17–23. <https://doi.org/10.1016/j.actatropica.2013.10.013>.
- Yang, H.M., Macoris, M.L.G., Galvani, K.C., Andriguetti, M.T.M., Wanderley, D.M.V., 2009. Assessing the effects of temperature on the population of *Aedes aegypti*, the vector of dengue. Epidemiol. Infect. 137 (8), 1188–1202. <https://doi.org/10.1017/S0950268809002040>.
- Zhang, Q., Sun, K., Chinazzi, M., Pastore y Piontti, A.I., Dean, N.E., Rojas, D.P., Merler, S., Mistry, D., Poletti, P., Rossi, L., et al., 2017. Spread of Zika virus in the Americas. Proc. Natl. Acad. Sci. U. S. A. 114 (22), E4334–E4343. <https://doi.org/10.1073/pnas.1620161114>.